Argonne NATIONAL LABORATORY

Fuel Cell System Modeling and Analysis

R. K. Ahluwalia, X. Wang, J-K Peng, C. F. Cetinbas, and D. Papadias

DOE Hydrogen and Fuel Cells Program 2017 Annual Merit Review and Evaluation Meeting

Washington, D.C.

June 5-9, 2017

Project ID: FC017

Overview

Timeline

- Start date: Oct 2003
- End date: Open
- Percent complete: NA

Budget

- FY16 DOE Funding: $550 K
- Planned DOE FY17 Funding: $500 K
- Total DOE Project Value: $500 K

Barriers

B. Cost

C. Performance

E. System Thermal and Water Management

F. Air Management

J. Startup and Shut-down Time, Energy/Transient Operation

Partners/Interactions

- Eaton, Ford, UDEL/Sonijector
- SA, Aalto University (Finland)
- 3M, Ballard, Johnson-Matthey Fuel Cells (JMFC), UTRC, FC-PAD, GM
- IEA Annex 34
- Transport Modeling Working Group
- Durability Working Group
- U.S. DRIVE fuel cell tech team

- This project addresses system, stack and air management targets for efficiency, power density, specific power, transient response time, cold start-up time, start up and shut down energy

Objectives and Relevance

Develop a validated system model and use it to assess design-point, part-load and dynamic performance of automotive (primary objective) and stationary (secondary objective) fuel cell systems (FCS)

- Support DOE in setting technical targets and directing component development
- Establish metrics for gauging progress of R&D projects
- Provide data and specifications to DOE projects on high-volume manufacturing cost estimation

Impact of FY2017 work

- Projected 44.9 $/kW$_e$ FCS cost at high volume manufacturing and 0.126 g/kW$_e$ Pt content with high performance (HP) d-PtNi/C cathode catalyst, reinforced 14-μm 850 EW membrane, and $Q/\Delta T$ = 1.45 kW/^{o}C constraint
- Estimated 10% degradation in net FCS power with 40% decrease in d-PtNi/C cathode catalyst ECSA (0.05-0.15 mg/cm^2 Pt loading) due to cyclic potentials
- Showed the possibility of removing cathode humidifier if MEA membrane thickness is <14-μm thin, and stack inlet pressure is 2.5 atm or higher
- Demonstrated through a CFD model that H_2 recirculation blower can be eliminated by using a pulse ejector and maintaining <20% N_2 mole fraction to avoid fuel starvation
- Evaluated extreme conditions (cell voltage, manufacturing volume, $Q/\Delta T$ constraint) where high stack inlet pressures (4 atm) may offer advantages

Q: Stack heat load; ΔT: Stack coolant exit T – Ambient T

Approach

Develop, document & make available versatile system design and analysis tools

- GCtool: Stand-alone code on PC platform
- GCtool-Autonomie: Drive-cycle analysis of hybrid fuel cell systems

Validate the models against data obtained in laboratories and test facilities inside and outside Argonne

- Collaborate with external organizations

Apply models to issues of current interest

- Work with U.S. DRIVE Technical Teams
- Work with DOE contractors as requested by DOE

1	Evaluate the performance of MEAs with de-alloyed PtNi/C cathode catalyst relative to the targets of 0.44 A/mg-PGM mass activity at 900 $mV_{iR\text{-}free}$, 1000 mW/cm^2 at rated power, and 300 mA/cm^2 at 800 mV.	12/16
2	Determine the comparative performance of four state-of-the-art MEAs with Pt, Pt-alloy and dealloyed Pt-alloy catalysts and electrode structures.	03/17
3	Model, update and project the durability of SOA catalysts and MEAs relative to the 2020 operating life target of 5000 h.	06/17
4	Update the performance and cost of an automotive fuel cell system with an advanced low-PGM catalyst relative to 2020 targets of 65% peak efficiency, $Q/\Delta T$ of 1.45 kW/K, and \$40/kW cost.	09/17

Technical Accomplishments: Summary

Stack: Collaboration with 3M, JMFC/UTRC, Ballard, FC-PAD and GM in obtaining data to develop validated models for pressures up to 3 atm

- Dispersed Pt/C and de-alloyed PtNi/C catalyst systems
- De-alloyed PtNi/C catalyst system: durability on drive cycles
- De-alloyed Pt_3Ni_7/NSTF catalyst system
- Dispersed PtCo/C alloy catalyst systems

Air Management: Investigating integrated air management system with two-stage, high speed centrifugal compressor and air-foil bearings (Honeywell patent)

Water Management: Optimized cost of integrated PEFC stack and cross-flow humidifier

- Investigated FCS performance without cathode humidifier (3M collaboration)

Fuel Management: Evaluating the performance of anode system with a pulse injector in lieu of H_2 recirculation blower (collaboration with Ford & UDEL)

Thermal Management: Optimizing system performance and cost subject to Q/ΔT constraint

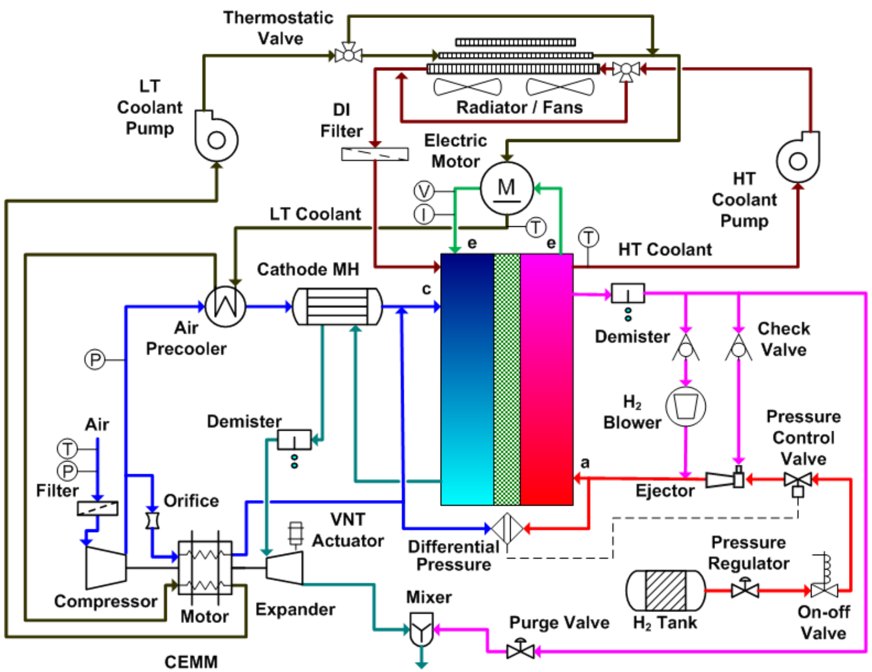

Argonne 2016 FCS

ΔT: Stack coolant exit T – Ambient T

From Differential Data to Integral Cell Model

1.1 Differential Cell Data
Variables: P, T, RH, X_{O2}, i

1.2 EIS Data

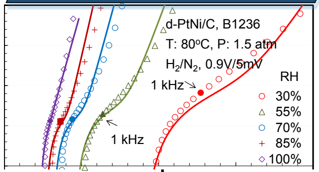

CCL Conductivity
σ_c (T, RH)

1.3 CV Data

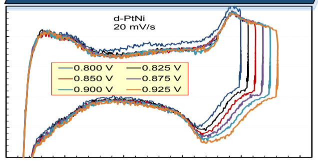

PtO$_x$ Formation
Θ(E)

2. Overpotential Breakdown
η_s^c, η_s^a, iR_Ω^m, iR_Ω^c, η_m

3. η_m Correlation
i_L(P, T, RH, X_{O2})
η_m(P, T, RH, X_{O2}, i/i_L)

FC-PAD

4. Expanded Polarization Data

5. Mass Transfer Resistance
R_m (P, T, RH, X_{O2}, E, i)

6. Resistance Breakdown
R_d: Pressure Dependent
R_{cf}: Pressure Independent

Gas Resistance
R_g(P,T,RH,X_{O2})

GDL Resistance
ε_τ^d, ε_τ^w(E, i), δ_l/δ_d

CCL Resistance
R_{cf} (T, RH, E, i)

Operating Conditions

7. Integral Cell Model
1+1D or 2+1D

Cell Design

Differential Cell Data

UTRC 12.25-cm^2 active area cell, triple serpentine flow channels, fixed flow rate 1(a) / 3(c) slpm, 5 minutes hold per point

- JMFC Catalyst: d-PtNi/C, 0.1 mg/cm^2 Pt loading, 60 m^2/g$_{Pt}$ ECSA (A_{Pt})
- BOL diagnostics: H_2-pump, H_2-xover, CV, EIS

Test Series	Tests	1	2	3	4	5	X_{O2}, %
1. Effect of P	P, atm	1	1.5	2.5			100, 21, 10, 6, 2, 1
2. Effect of T	T, °C	90	80	70	60	45	100, 21
3. Effect of RH	Φ, %	100	85	70	55	30	100, 21, 10

Electrode conductivity (σ_c) from Galvanostatic impedance data for H_2/N_2 at 0.4 to 0.925 V with 5 mV perturbation

- σ_c has similar temperature and RH dependence as σ_m: $\sigma_c = \sigma_m f(\varepsilon_i, \tau)$

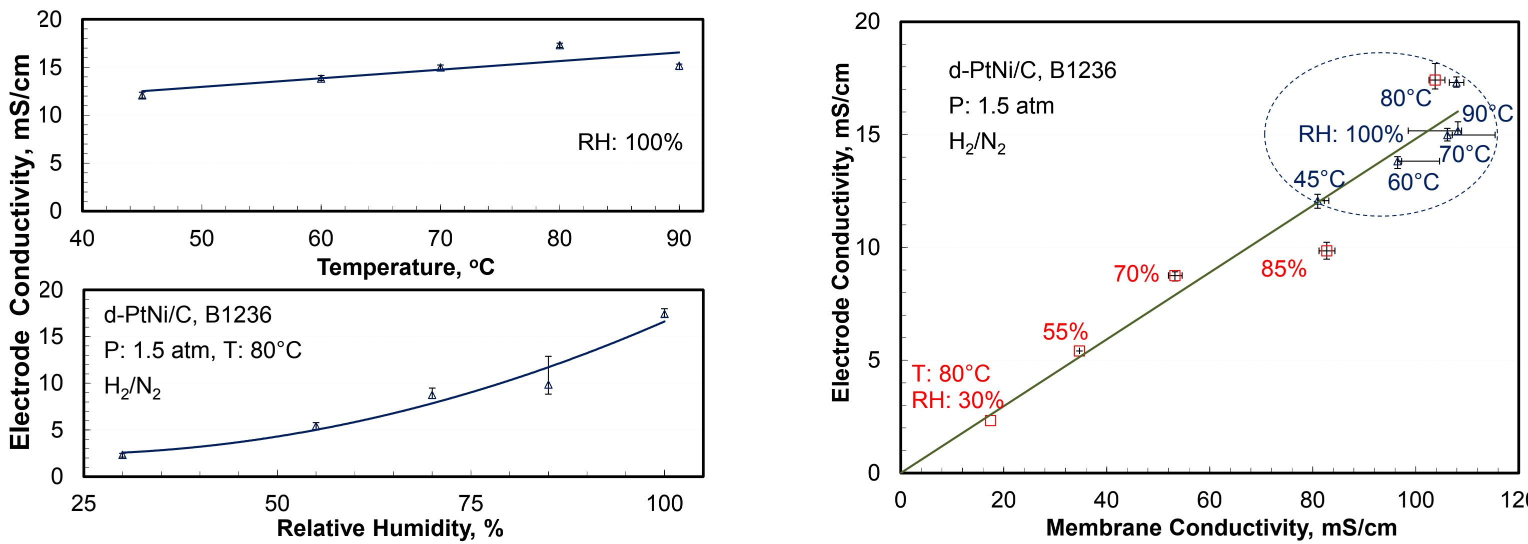

σ_m; Membrane conductivity; ε_i : Ionomer volume fraction; τ; Tortuosity for ion conduction

ORR Kinetics for d-PtNi/C Catalyst MEA

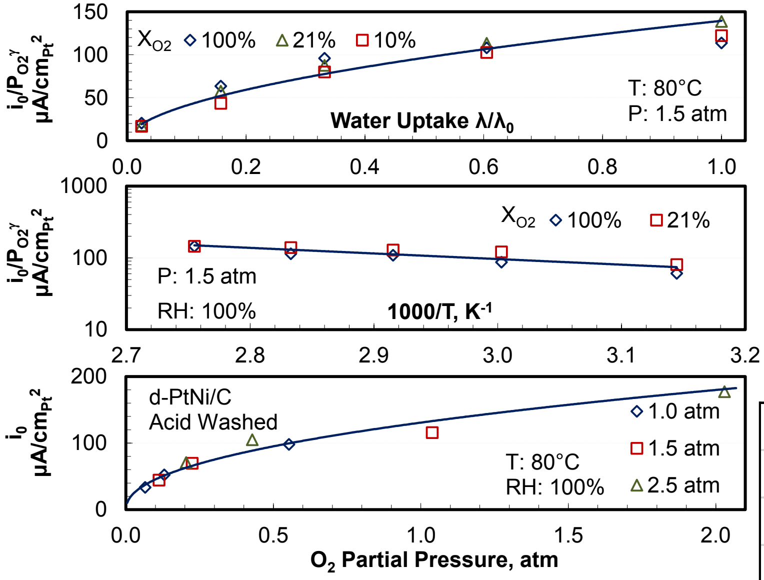

Distributed ORR kinetic model

$$\eta_c = \eta_s^c + iR_\Omega^c \left(\frac{i\delta_c}{b\sigma_c}\right)$$

$$i = i_0(1-\theta)e^{-\frac{\omega\theta}{RT}}e^{\frac{\alpha nF}{RT}\eta_s^c}$$

$$i_0 = i_{0r}e^{-\frac{\Delta H_S^c}{RT}\left(\frac{1}{T}-\frac{1}{T_r}\right)}P_{O_2}^{\gamma}\left(\frac{\lambda}{\lambda_0}\right)^{\beta}$$

	Ionomer		Cathode	Mass Activity	
Cathode Catalyst	**EW (I/C)**	**L_{Pt}(c)**	**ECSA**	**Data**	**Model**
		mg/cm^2	m^2/g	A/g_{Pt}	A/g_{Pt}
Dispersed De-alloyed Catalyst (FC106, 12.25-cm^2 cell)					
d-$PtNi_3$/C	850 (1.0)	0.1	64±11	500±100	650±120
Baseline Annealed Pt Catalysts (FC106, 12.25-cm^2 cell)					
a-Pt/C	1100 (0.8, 1.2)	0.104	48±4	312±24	319±30
Baseline Dispersed Pt Catalysts (FC106, 12.25-cm^2 cell)					
Pt/C	1100 (0.8)	0.092	90±8	432±22	456
Dispersed PtCo Catalysts (FC-PAD, 50-cm^2 cell)					
$Pt_{60}Co_{40}$/C	(0.34)	0.21	42.4	745	763
$Pt_{70}Co_{30}$/C	(0.9)	0.1	42.4±0.7	659	623
$Pt_{85}Co_{15}$/C	(0.9)	0.1	42.4	760	661
NSTF Catalysts (FC104, 50-cm^2 cells, 5-cm^2 for binary catalyst with CI)					
$Pt_{68}(CoMn)_{32}$/NSTF	None	0.1	9.8	180	190
d-Pt_3Ni_7/NSTF	None	0.125	14.5±0.7	330±30	392
d-Pt_3Ni_7/NSTF + Cathode Interlayer (CI)	None	0.096 + 0.016 (CI)	22±3	380±60	334

- d-PtNi/C has 2X modeled mass activity of a-Pt/C that has nearly the same particle size
- d-PtNi/C and PtCo/C alloy have comparable mass activities
- Both d-PtNi/C and PtCo/C alloy systems meet the mass activity targets of 440 A/g_{Pt}

Mass Transfer Overpotentials

Determined limiting current density (i_L) and correlated mass transfer overpotential (η_m) with reduced current density (i/i_L)

- Mass transfer overpotentials derived from pol curves do not correlate with mass activity

  $$\eta_m = E_N - E - iR_\Omega^m - \eta_c - \eta_a$$

- i_L defined as current density at which η_m = 450 mV
- Limiting current densities are higher and mass transfer overpotentials are lower in NSTF MEAs than in dispersed catalyst MEAs with nearly same Pt loading

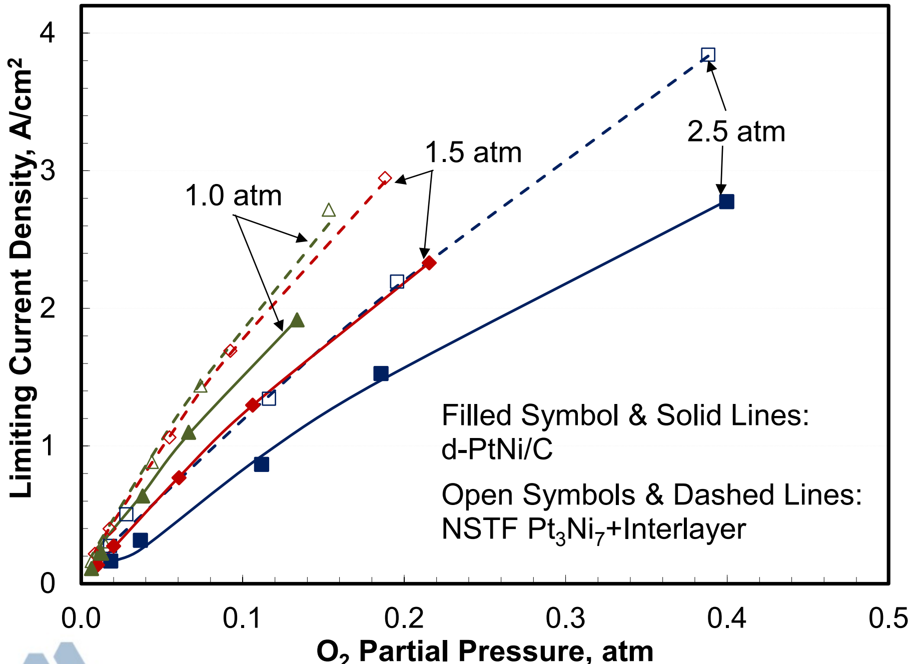

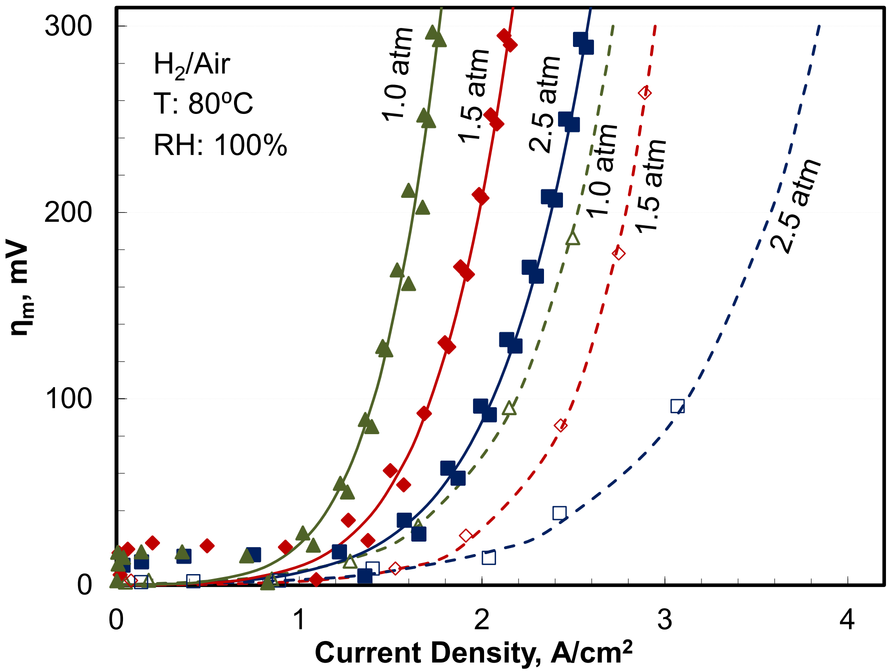

Model Calibration: Stack with d-PtNi/C Cathode Catalyst

High performance (HP) stack with d-PtNi/C cathode catalyst, 10°C rise in coolant T (ΔT_c)

- 0.025(a)/0.1(c) mg/cm^2 Pt loading
- 850 EW, 14-μm (dry) chemically-stabilized, reinforced membrane, ~42 mΩ.cm^2 HFR(1)
- 20% higher i_L reflecting better high surface-area carbon support (FC144)
- 47 mΩ.cm^2 electrode sheet resistance ($^{\delta_c}/_{\sigma_c}$) at 100% RH

Sources of Cell-to-Stack Derating in Power Density at Q/ΔT Relevant Conditions

2.5-atm Stack Inlet P, 95°C Stack T(2)

- Operating pressure, 2.5 atm inlet (i) vs. 2.5 atm outlet (o): 4.4%
- Air stoichiometry (SR(c)), 1.5 vs. 2.0: 7.3%
- Total derating: 11.3%

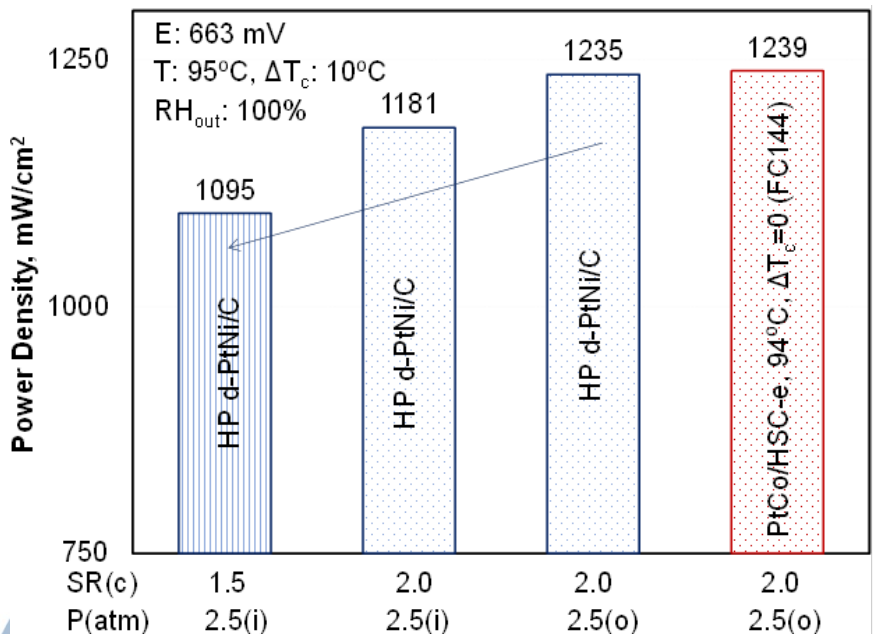

1.5 Stack Inlet P, 95°C Stack T(2)

- Operating pressure, 1.5 atm inlet vs. 1.5 atm outlet: 8.7%
- Air stoichiometry, 2.5 vs. 1.5: 6.9%
- RH_{in}, 51% vs. 70%: 2.3%

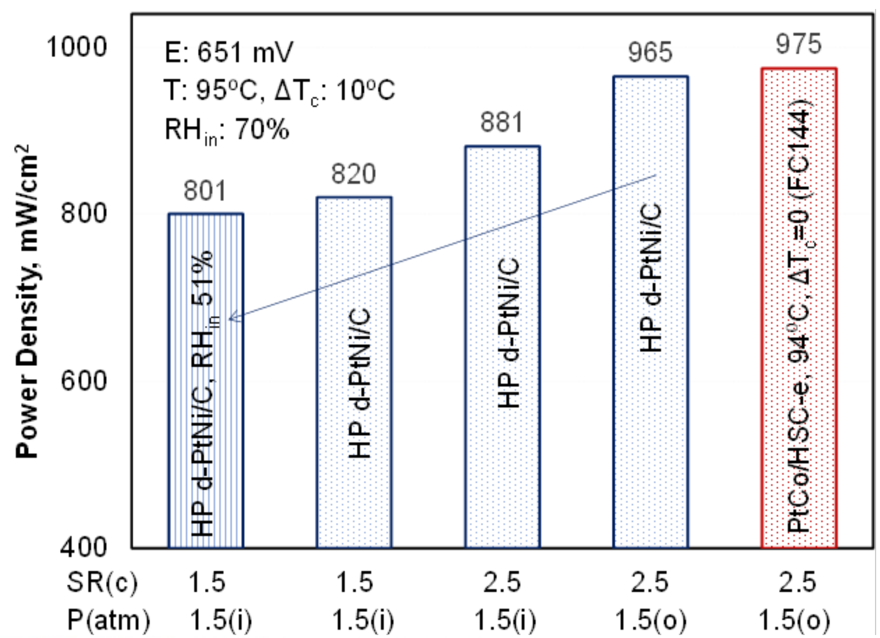

(1)High-frequency resistance for 2.5-atm conditions; (2)Bipolar plate temperature at coolant exit

Projected Performance of Automotive FCS: HP d-PtNi/C Cathode Catalyst

Modeled optimal beginning of life (BOL) performance of automotive FCS subject to Q/ΔT=1.45 kW/°C constraint: 0.125 mg/cm² total Pt loading; 850 EW, 14-µm chemically-stabilized, reinforced membrane

- Projected FCS cost and Pt content: 44.9 $/kW$_e$ at 2.5 atm, and 0.126 g$_{Pt}$/kW$_e$ at 2.5-atm stack inlet pressure, 95°C stack temperature
- Determined Optimum exit RH: ~100% at 2.5 atm and <60% at 1.5 atm

T: 95°C		Stack Gross				FCS Net	
P	CEM Power	Current Density	Cell Voltage	Power Density	Stack Pt Content	Pt Cost	Stack Cost
atm	kW$_e$	A/cm²	mV	mW/cm²	g$_{Pt}$/kW$_e$	$/kW$_e$	$/kW$_e$
3.0	8.8	1.735	670	1162	0.108	5.8	18.6
2.5	7.0	1.651	663	1095	0.114	6.1	19.2
2.0	5.5	1.457	657	956	0.131	6.8	21.1
1.5	4.1	1.231	651	801	0.156	8.0	24.2

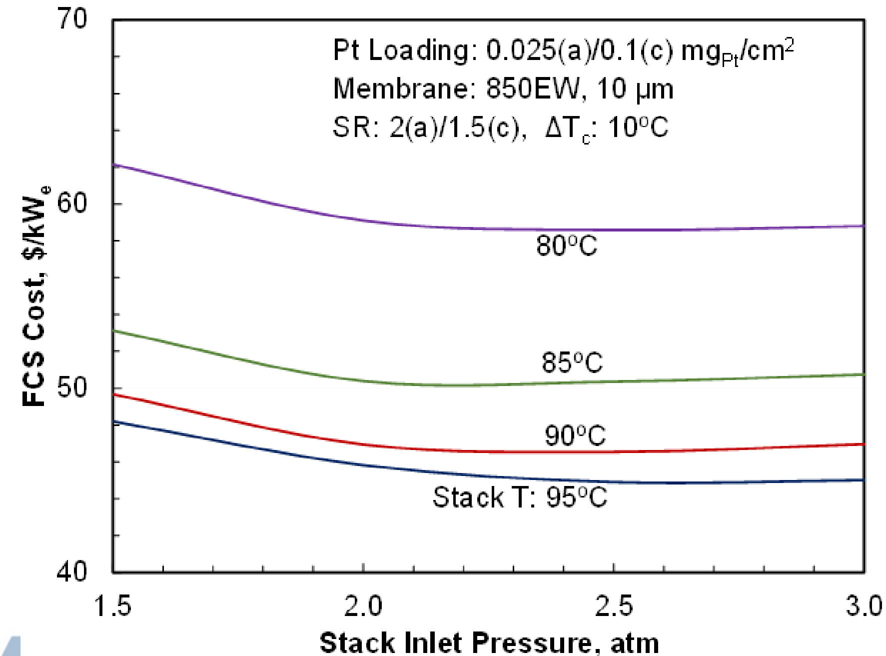

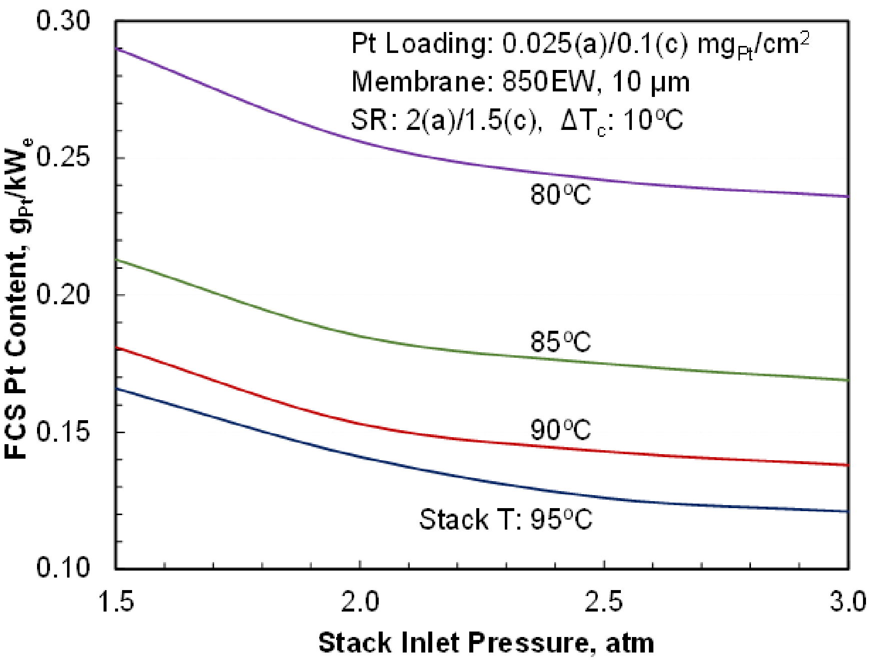

Cost correlations from Strategic Analysis (SA), 500,000 units/year, no H_2 blower

Optimum Pt Loading in HP d-PtNi/C Cathode Electrode*

Similar total overpotentials but current density is lower at lower Pt loadings in cathode (L_{Pt}(c)), 663-mV cell voltage

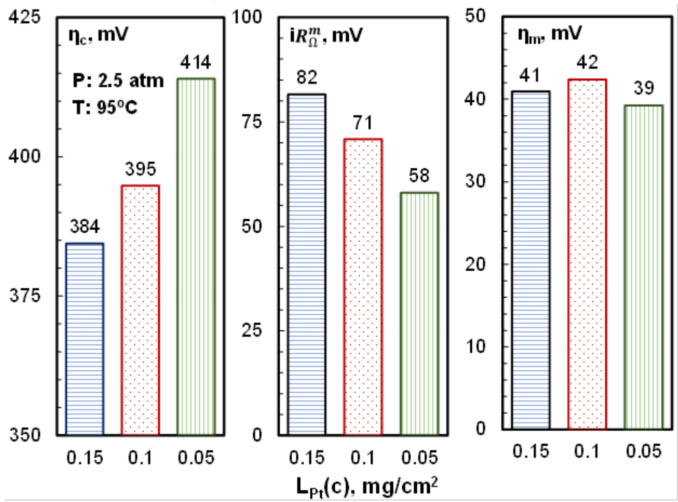

Similar total overpotentials at 1.5 atm as at 2.5 atm but at much lower current densities, 651-mV cell voltage

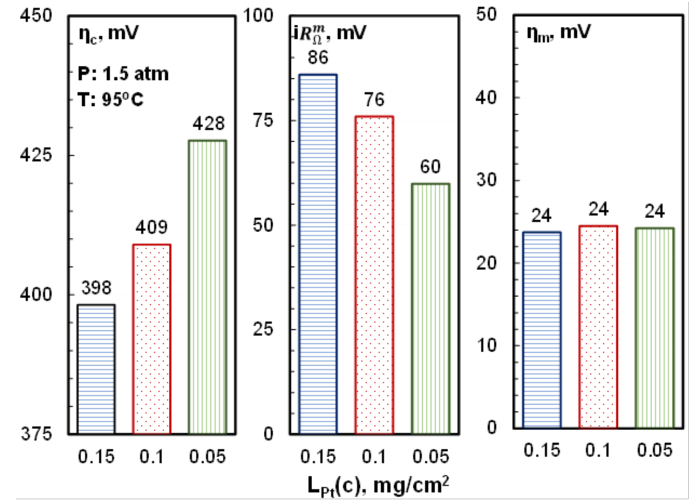

~33% lower power density at 0.05 mg/cm² Pt loading in cathode

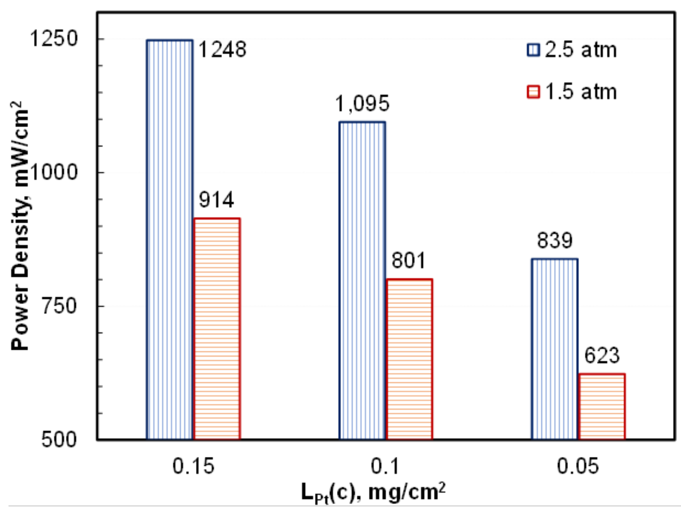

Small differences in FCS cost may favor >0.10 mg/cm² Pt loading in cathode

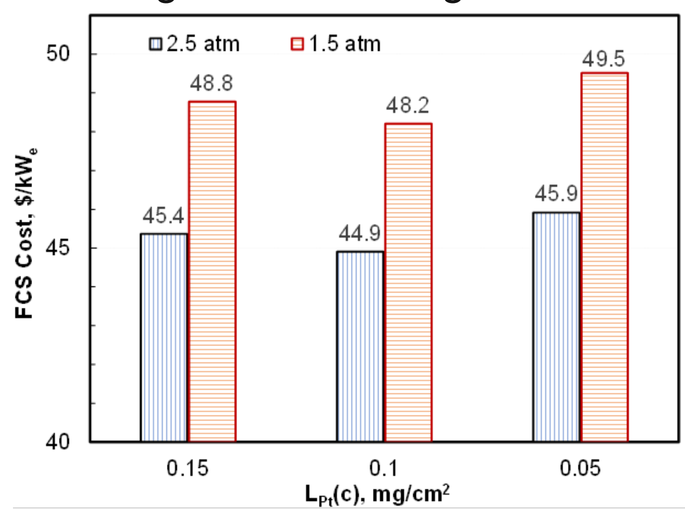

*Conditions as in slide 10, $Q/\Delta T$=1.45 kW/°C, 95°C stack T, ΔT_c = 10°C

Stability of d-PtNi/C Electrode under Cyclic Potentials

Collaboration with FC-106: Catalyst AST, 30,000 cycles

- Measured ECSA loss higher on trapezoid cycles (0.6-0.95 V, 700 mV/s) than on triangle cycles (0.6-925 V, 50 mV/s)
- Faster ECSA loss with extensive intra-cycle diagnostics
- WAXS indicates extensive leaching of Ni that depends on duty cycle[1]

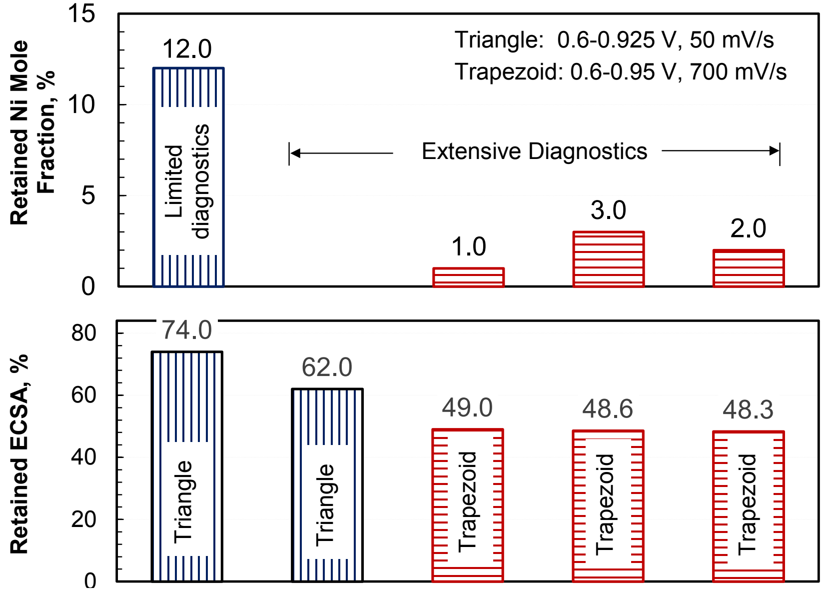

<10% decrease in specific activity even with >90% Ni loss from alloy catalyst

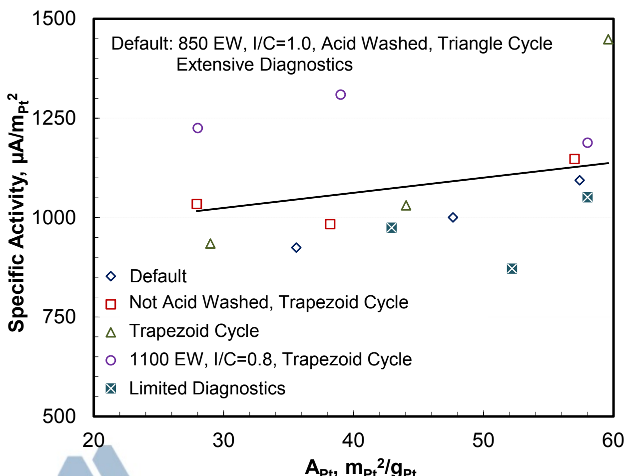

Linear correlation between mass activity and ECSA

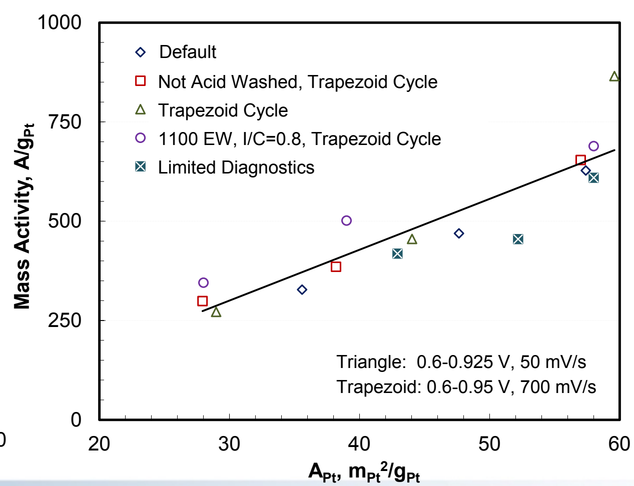

Correlation between limiting current density and Pt surface roughness (S_{Pt})

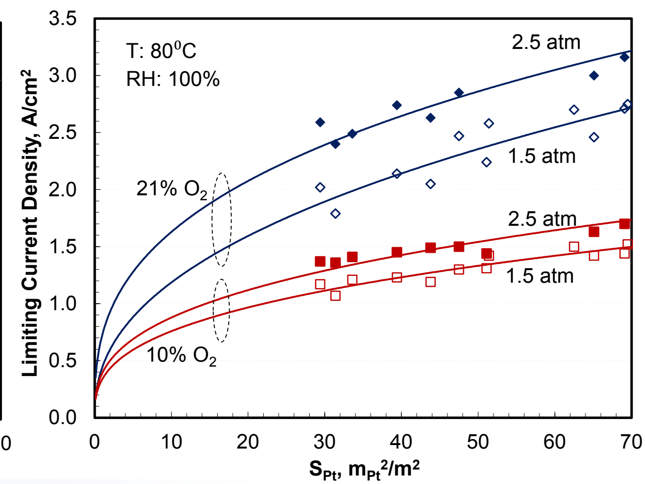

1) WAXS data from N. Kariuki and D. Myers (ANL)

Projected FCS Performance Degradation

To meet the target of 10% derating in net FCS power over lifetime, the acceptable ECSA loss (ΔA_{Pt}) is limited to <40% for L_{Pt}(c)=0.1 mg/cm^2

- Small dependence of acceptable ECSA loss on Pt loading (L_{Pt}) although Pt loading may affect ECSA loss over cyclic potentials and startup/shutdown
- Regardless of Pt loading, increase in kinetic and mass transfer overpotentials contribute equally to voltage loss
- Additional degradation mechanisms involving other components (membrane, catalyst support) and fuel/air impurities to be included in future work

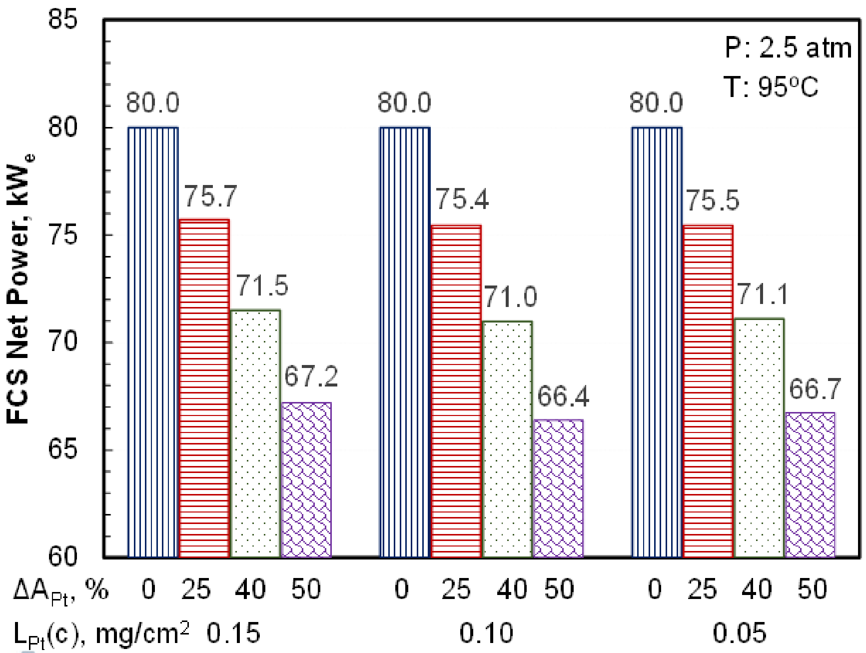

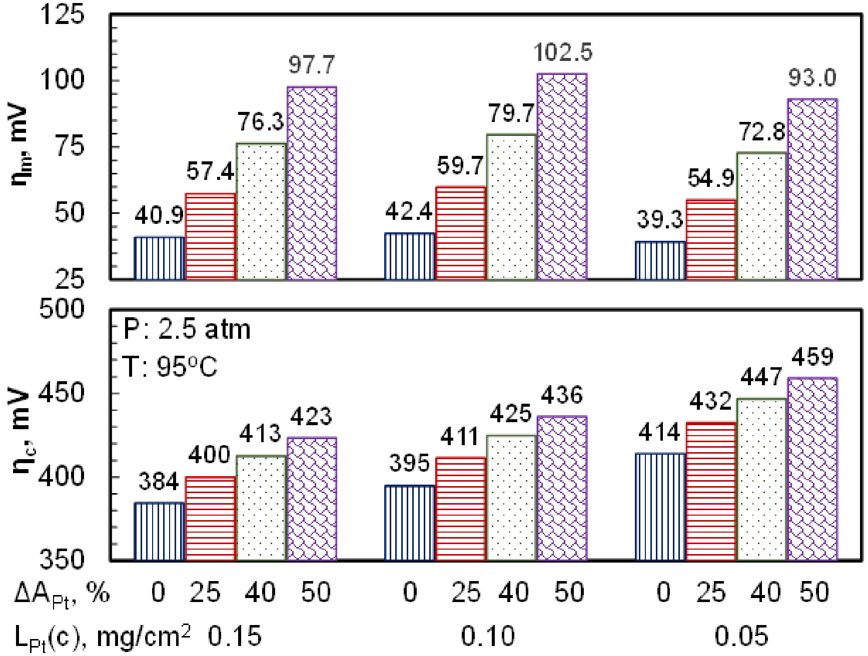

Water Management System

Collaborated with 3M (FC104) to design and conduct tests analyzing the effects of anode and cathode RH on performance of 5-cm^2 active-area differential cells

- Anode: Ternary $Pt_{68}(CoMn)_{32}$, 0.019 mg_{Pt}/cm^2
- Cathode: Binary Pt_3Ni_7/NSTF, 0.096 mg_{Pt}/cm^2, with 3M Type "B" cathode interlayer, 0.016 mg_{Pt}/cm^2
- Membrane: 3M-S (reinforced) 725 EW PFSA with additive, 14 μm
- Diffusion Media: 3M "X3" cathode GDL (experimental backing, MPL), 3M 2979 cathode GDL

Developed models for effect of anode RH on HFR, ORR kinetics, limiting current and mass transfer overpotential

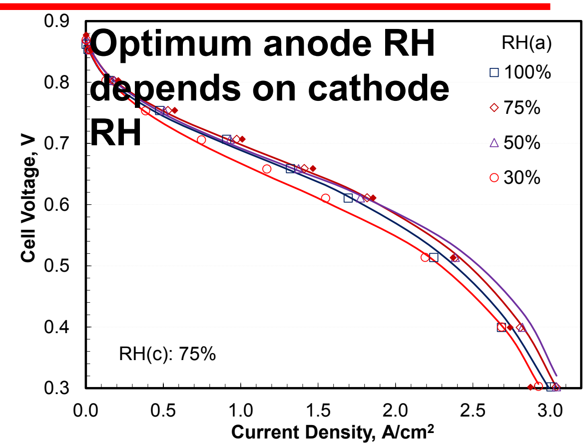

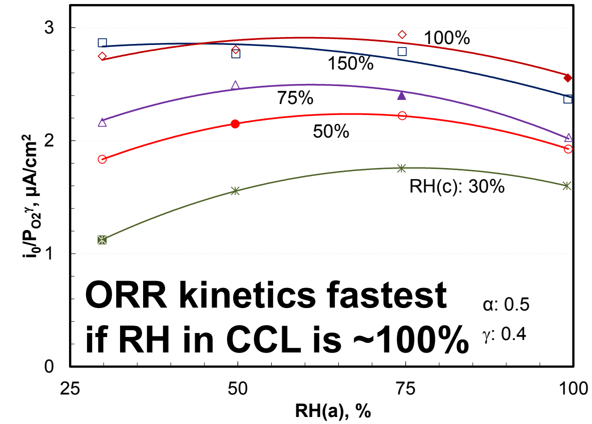

Lower HFR under wet conditions

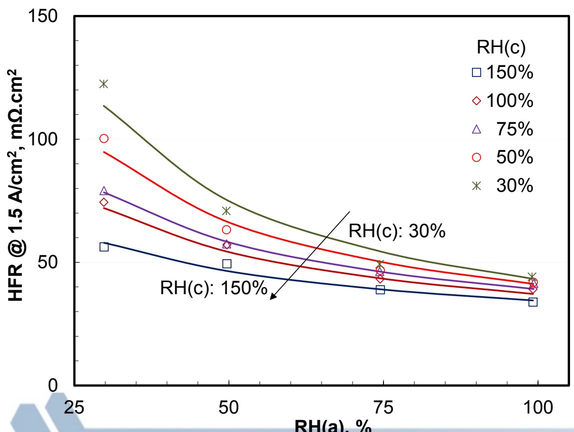

Lower limiting current density under wet conditions

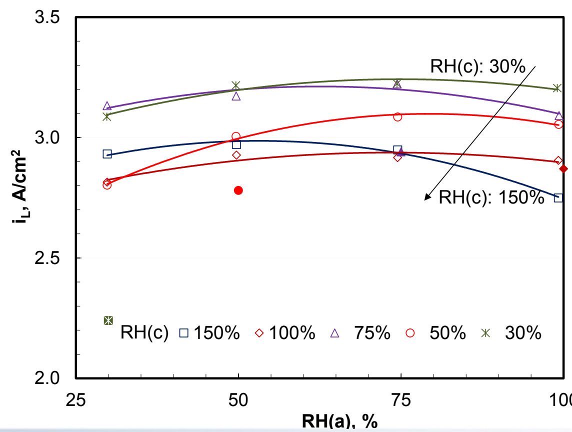

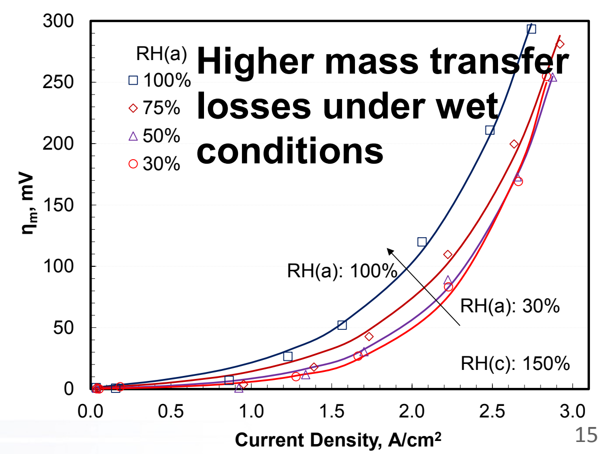

All results for H_2/Air, P = 1.5 atm, T = 80^{o}C

Water Transport in FCS w/o Cathode Humidifier

Self humidification of cathode by internal water transport from anode to cathode (and vice versa) across thin (14 μm) membrane

- Complete water balance at steady state: zero net transport
- Exit cathode RH is only a function of cell temperature and cathode SR
- Exit anode RH depends on cell temperature and anode SR

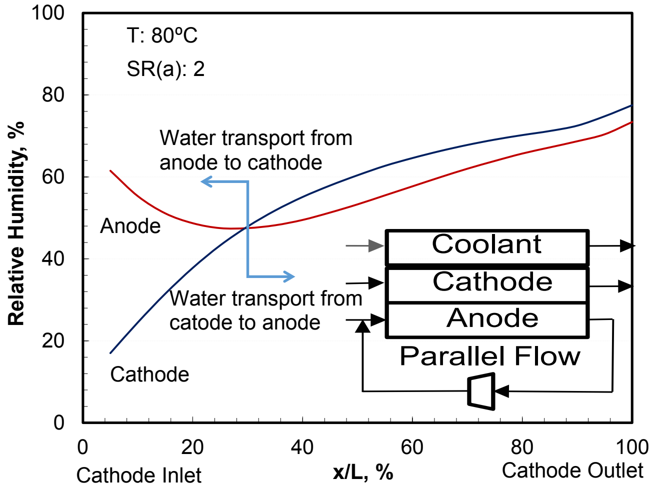

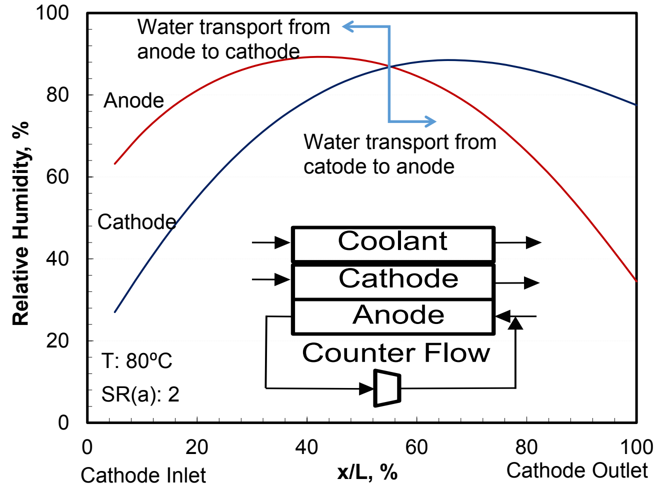

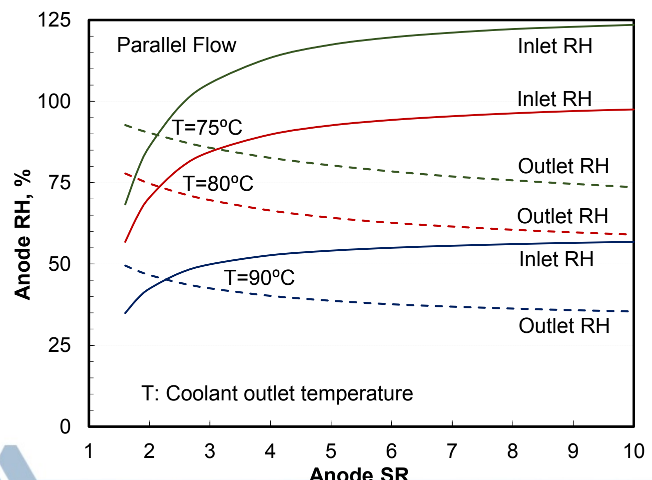

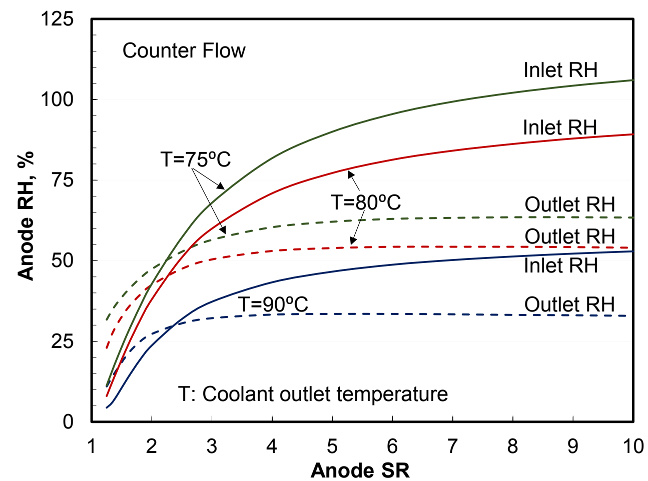

- Coolant flow concurrent with cathode flow
- Cathode inlet and outlet RHs do not depend on anode flow but cathode RH distribution depends on whether anode flow is co-flow or counter-flow

P	1.5 atm	
ΔT_c	10^oC	
SR(c)	1.5	
T	RH(c) In	RH(c) Out
75^oC	22%	92%
80^oC	18%	75%
85^oC	14%	61%
90^oC	12%	51%

Performance of FCS w/o Cathode Humidifier

All results for fixed 0.675 cell V, $\Delta T=10^oC$, SR(c)=1.5

Effect of cathode humidifier on stack power density

- Small improvement at low cell temperature
- Larger improvement at low operating pressure
- Larger improvement for parallel flow

Conclusions

- Cathode humidifier needed at 1.5 atm and >90°C, especially with parallel flow
- Small penalty in removing humidifier at 2.5 atm, especially with counter flow

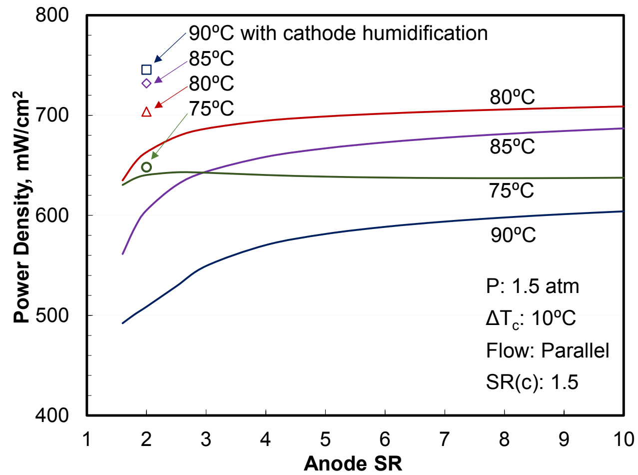

Power density decreases if SR(a) < 2, but parasitic power too high if SR(a) > 2

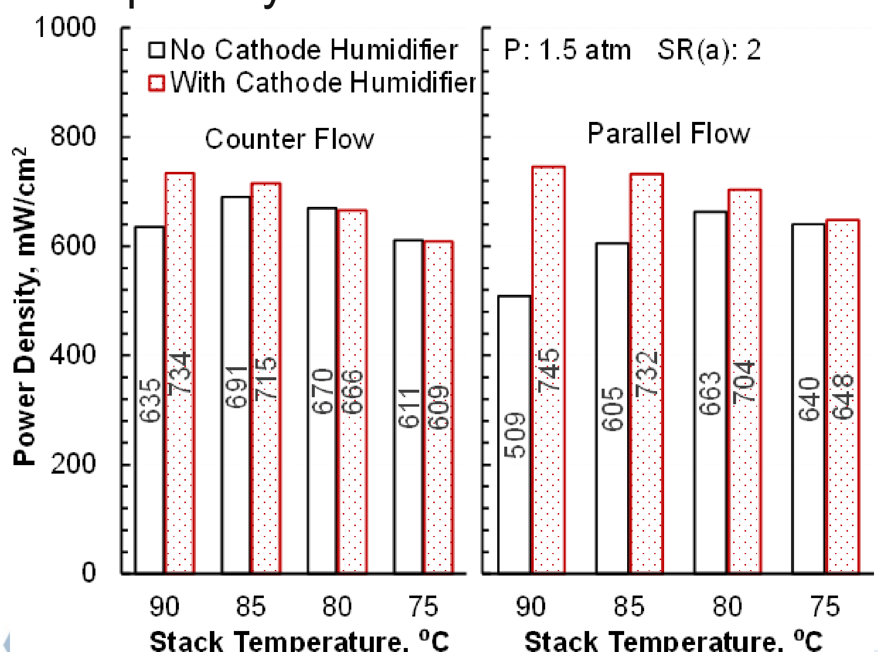

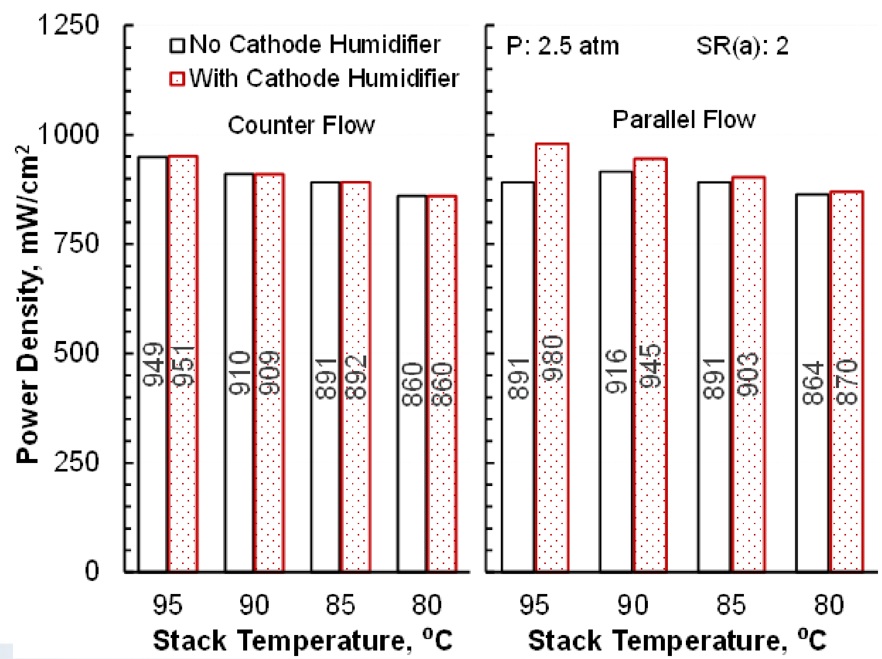

Fuel Management System

Comparing fixed/variable area twin ejectors, hybrid ejector-recirculation pump, and pulse ejector[1]

- CFD model of H_2 ejector with converging-diverging nozzle, undergoing testing and validation
- Process model of supersonic ejector with normal and oblique shocks, calibrated with laboratory data
- CFD model of pulse ejectors

Hybrid system with variable-area nozzle ejector (but not two-parallel ejectors) can meet flow and H_2 stoichiometry targets

Cost of recirculation blower: ~3.25 $/kW_e$

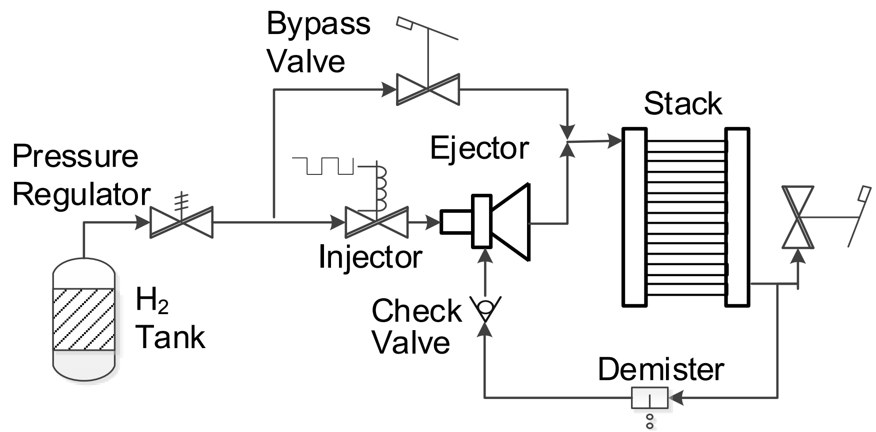

Pulse Ejector based Anode System

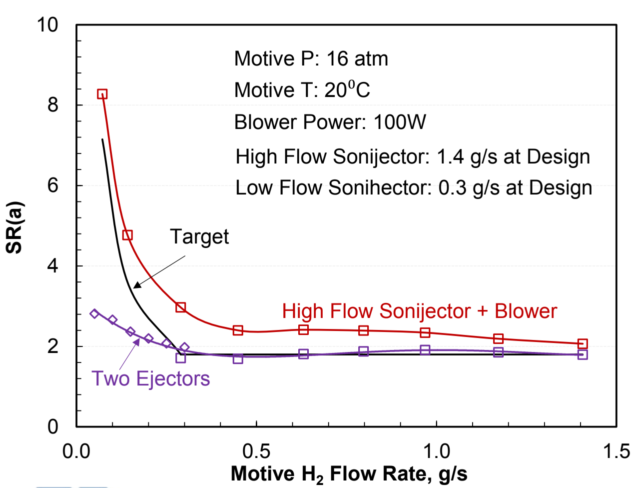

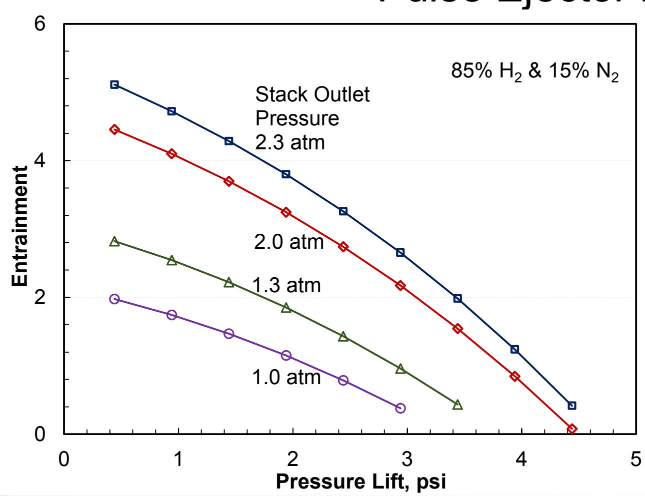

Modeled operating map of a fixed-area ejector with constant motive gas pressure (10.7 atm) and H_2 flow rate (1.38 g/s). Variable suction/delivery pressure

Entrainment: Ratio of suction to motive gas mass flow rate

R. Senner, D. Di Fiore, Injector Control for Fuel Cell System, GM Patent, US 8,389,168, 2013

Performance of Pulse Ejectors

Pulses of stack inlet/outlet pressure generated by opening (10 ms) and closing (90 ms) of H_2 injector

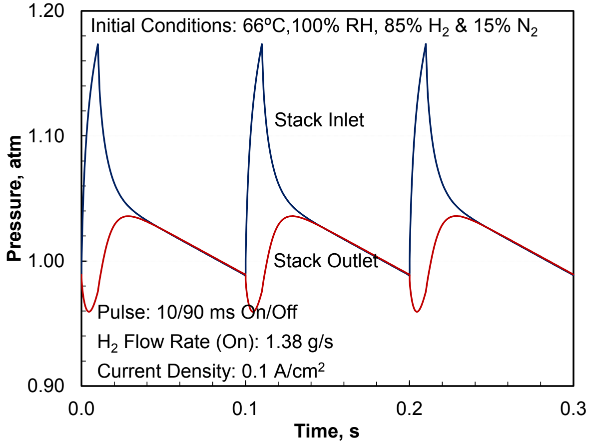

Periodic variation of H_2 mole fraction, 0.1 A/cm^2 current density; H_2 on for 5 ms, off for 45 ms

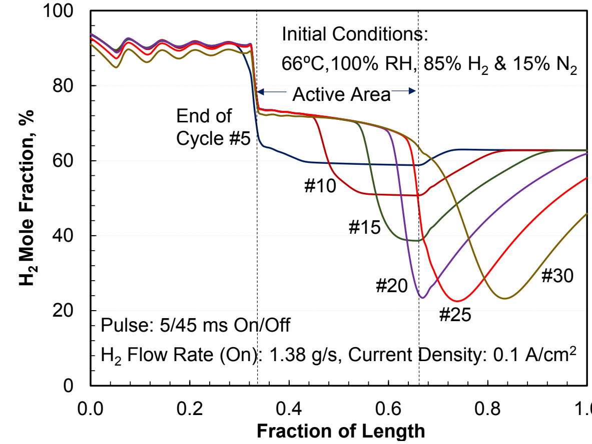

Depending on pulse width/frequency, there is threshold N_2 content for H_2 starvation at low current densities

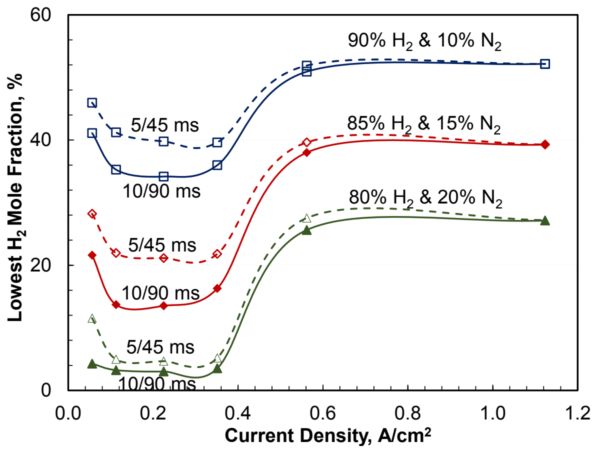

Peak gas velocity depends on pulse width and controls the ability to remove liquid water and prevent its accumulation

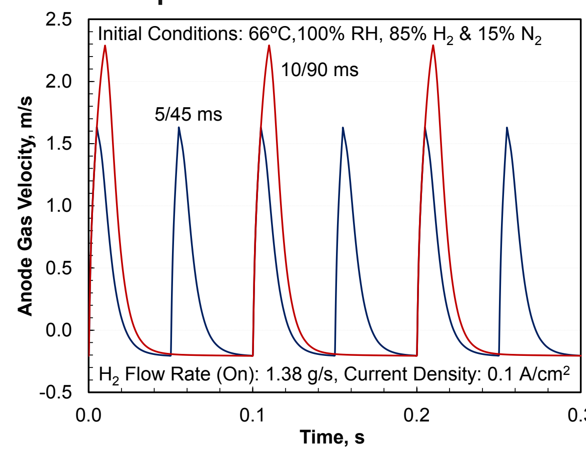

Conclusion: May be feasible to replace hybrid ejector-recirculation pump with a pulse ejector, with limits on allowable N_2 build-up and pulse width

Air Management System

Study Objective: Evaluate possible advantage of air management system capable of delivering air at high pressures, up to 4 atm

2-Stage Centrifugal Compressor

- Mixed axial and flow compressors on a common shaft with air foil bearings (AFB); Honeywell US Patent 2015/0308456
- 3-phase brushless DC motor, liquid and air cooled; liquid-cooled motor controller
- Compressor power >20 kW_e needed even if AFB/motor cooling air is recovered

FCS Performance at 4-atm Stack Inlet P

- 5.3% increase in MEA power density if Q/ΔT constraint is imposed, SR(c)=1.5, 0.718 V required cell voltage
- 25% increase in MEA power density at the 2.5-atm operating cell voltage, 0.672 V
- At low manufacturing volume, 1000 units/year, the cost of 4-atm FCS is only 3.8% higher at same cell voltage, 0.672 V

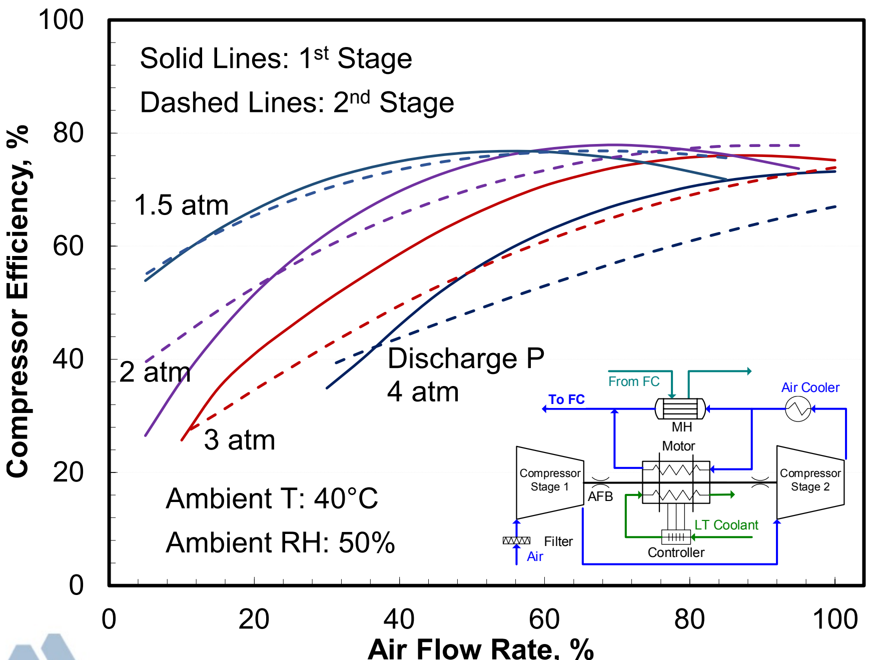

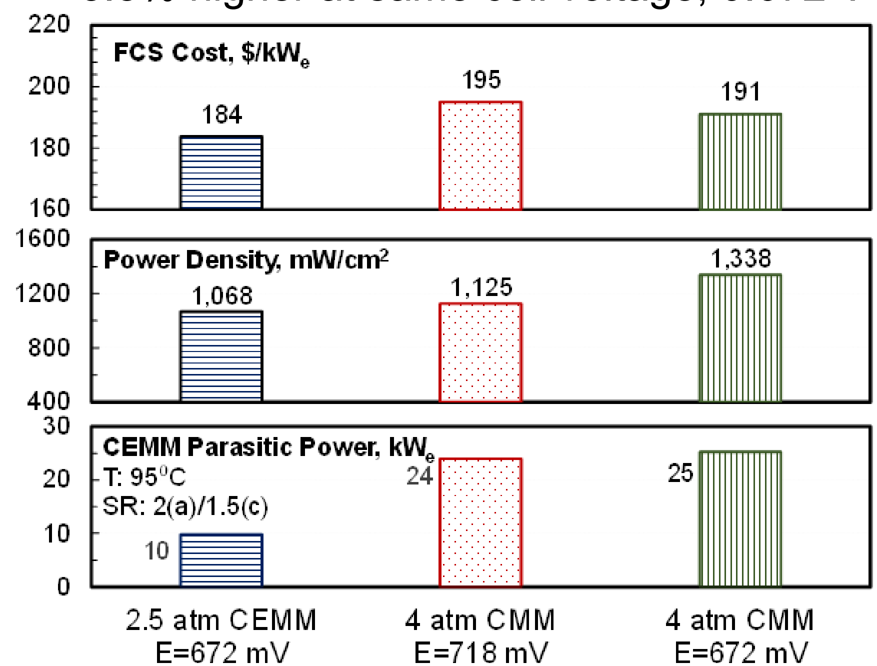

Cost correlations from SA, 1,000 units/year, Ejector + H_2 blower

Collaborations

Air Management	Eaton: Roots Air Management System with Integrated Expander (FC103)
Stack	3M: High Performance, Durable, Low Cost Membrane Electrode Assemblies for Transportation (FC104) Ballard/Eaton: Roots Air Management System with Integrated Expander (FC103) JMFC and UTRC: Rationally Designed Catalyst Layers for PEMFC Performance Optimization (FC106)
	FC-PAD: Fuel Cell Performance and Durability Consortium (FC135, FC136, FC137, FC138, FC139) GM: Durable High-Power Membrane Electrode Assemblies with Low Pt Loadings (FC156)
Water Management	Gore, Ford, dPoint: Materials and Modules for Low-Cost, High-Performance Fuel Cell Humidifiers (FC067)
Thermal Management	3M, Honeywell Thermal Systems
Fuel Management	3M, University of Delaware (Sonijector)
Fuel Economy	ANL-Autonomie (SA044), Aalto University (Fuel Cell Buses)
H_2 Impurities	3M
System Cost	SA: Manufacturing Cost Analysis of Fuel Cell Systems and Transportation Fuel Cell System Cost Assessment (FC163)
Dissemination	IEA Annex 34, Transport Modeling Working Group, Durability Working Group, Catalyst Working Group

- Argonne develops the fuel cell system configuration, determines performance, identifies and sizes components, and provides this information to SA for high-volume manufacturing cost estimation

Proposed Future Work

1. Support DOE development effort at system, component, and phenomenological levels
2. Support SA in high-volume manufacturing cost projections, collaborate in life-cycle cost studies
   - Optimize system parameters considering costs at low-volume manufacturing
   - Life cycle cost study for fuel cell electric buses (work with Ballard, Eaton, SA)
3. Alternate MEAs with advanced alloy catalysts
   - State-of-the-art low PGM Pt and Pt alloys (FC-PAD collaboration)
   - De-alloyed PtNi on high surface-area carbon support (ANL catalyst project with JMFC and UTRC as partners), calibrate/validate model on larger area cells
   - Alternate electrode structures (FC-PAD FOA projects collaboration)
4. System architecture and balance-of-plant components
   - Air management system with centrifugal and Roots compressors and expanders (Honeywell/Eaton collaboration)
   - Fuel and water management systems: anode gas recirculation, internal/external humidification
   - Bipolar plates and flow fields for low pressure drops and uniform air/fuel distribution, cell to stack performance differentials
5. Incorporate durability considerations in system analysis
   - System optimization for cost, performance, and durability on drive cycles (Advanced alloy catalyst systems)

Project Summary

Relevance:	Independent analysis to assess design-point, part-load and dynamic performance of automotive and stationary FCS
Approach:	Develop and validate versatile system design and analysis tools Apply models to issues of current interest Collaborate with other organizations to obtain data and apply models
Progress:	Projected 44.9 $\$/kW_e$ FCS cost and 0.126 g/kW_e Pt content with HP d-PtNi/C cathode catalyst, reinforced 14-μm 850 EW membrane, and $Q/\Delta T$ = 1.45 $kW/^oC$ constraint Estimated 11% degradation in net FCS power with 40% decrease in d-PtNi/C cathode catalyst ECSA (0.05-0.15 mg/cm^2 Pt loading) due to cyclic potentials Showed the possibility of removing cathode humidifier for MEA membrane thickness <14-μm thin, and stack inlet P >2.5 atm Demonstrated that H_2 recirculation blower can be eliminated with a pulse ejector and maintaining <20% N_2 mole fraction Evaluated favorable extreme conditions (cell voltage, volume of manufacturing, $Q/\Delta T$ constraint) for high stack inlet P (4 atm)
Collaborations:	3M, Aalto University, Eaton, JMFC, SA, UTRC, UDEL/Sonijector
Future Work:	Fuel cell systems with emerging high activity catalysts Alternate balance-of-plant components System analysis with durability considerations on drive cycles

Reviewers' Comments

Key recommendations and feedback

- Investigate dispersed systems, including PtCo catalysts
- Show parasitic losses for the air machine vs. inlet air pressure
- De-emphasize work on 3M nanostructured thin-film catalyst
- Closer cooperation with FC-PAD activities and projects
- Clarify interactions with SA, collaboration or source of cost correlations
- This is a good solid model and a good team

Work scope consistent with above recommendations

√ Focused work on d-PtNi/C dispersed catalysts using differential cell data obtained in collaboration with JMFC and UTRC (FC-106)

√ On-going work on differential cell data for PtCo/C dispersed catalysts in collaboration with FC-PAD and an industrial partner. Initial results on performance and durability are included in FC-PAD presentations. The PI is FC-PAD coordinator for modeling and validation thrust area.

√ Maintained and expanded collaborations with material and component developers and other projects

√ Investigating non-NSTF advanced catalysts, with emphasis on low PGM alloys

√ All system analysis work is based on 1D+1D or 2D+1D down-the-channel stack model, co- or counter-flowing anode and cathode streams, anode recycle, etc.

√ On-going parallel work on bipolar plates, flow fields, fuel system, alternate system architecture

√ ANL is a subcontractor to SA on FC-018 project, responsible for supplying performance and design data. Plans and recent results are discussed in bi-weekly calls.

Technical Back-Up Slides

Publications and Presentations

Journal Publications

R. K. Ahluwalia, X. Wang, and A. J. Steinbach, "Performance of Advanced Automotive Fuel Cell Systems with Heat Rejection Constraint," Journal of Power Sources, Vol. 309, pp. 178-191, 2016.

R. K. Ahluwalia, J.-K. Peng, X. Wang, D. A. Cullen, and A. J. Steinbach, "Long-Term Stability of Nanostructured Thin Film Electrodes at Operating Potentials," Journal of the Electrochemical Society, Vol. 164(4), pp. F306-F320, 2017.

F. C. Cetinbas, R. K. Ahluwalia, N. Kariuki, et. al., "Hybrid Approach Combining Multiple Characterization Techniques and Simulations for Microstructural Analysis of Proton Exchange Membrane Fuel Cell Electrodes," Journal of Power Sources, Vol. 344, pp. 62-73, 2017.

Conference Presentations

R. K. Ahluwalia, X. Wang, J-K Peng, and C. F. Cetinbas, "Fuel Cells Systems Analysis," US Drive Fuel Cell Tech Team Meeting, Southfield, MI, May 18, 2016.

C. F. Cetinbas, R. K. Ahluwalia, N. Kariuki, D. J. Myers, V. J. De Andrade, "Hybrid Approach for PEM Fuel Cell Electrode Microstructural Analysis," ElectroCat Workshop, Argonne National Laboratory, Argonne, IL, July 26, 2016.

D. Myers, N. Kariuki, R. Ahluwalia, X. Wang, C. F. Cetinbas, and J.-K. Peng, "Performance and Stability of MEA for PEMFC with Pt Alloy Cathode Catalyst," IEA Annex 34 Meeting, Beijing, China, Nov. 9, 2016.

R. K. Ahluwalia, V. Weißbecker, C. Wang, S. Hirano, H. Bramfeldt, and H. Ljungcrantz, "Bipolar Plates for Automotive Fuel Cells: Annex 34 Summary Report," IEA Annex 34 Meeting, Beijing, China, Nov. 9, 2016.

R. K. Ahluwalia, and N. Garland, "Reports from the Annexes: Annex 34," IEA AFC ExCo 53rd Meeting, Beijing, China, Nov. 10-11, 2016.

R. K. Ahluwalia, D. D. Papadias, X. Wang, R. Borup, R. Mukundan, M. Brady, J. Thompson, H. Wang, and J. Turner, "Modeling Performance and Stability of Bipolar Plates for Automotive Fuel Cells," DOE 2017 Bipolar Plates Workshop, Southfield, MI, Feb. 14, 2017.

R. Borup, R. Mukundan, T. Rockward, M. Brady, J. Thompson, D. D. Papadias, R. K. Ahluwalia, H. Wang, and J. Turner, "Metal Bipolar Plate Testing," DOE 2017 Bipolar Plates Workshop, Southfield, MI, Feb. 14, 2017.

Meetings Organized

R. K. Ahluwalia, "IEA Advanced Fuel Cells Annex 34: Fuel Cells for Transportation," Beijing, China, Nov. 9, 2016.

FCS with HP d-PtNi/C Cathode Catalyst: Critical Assumptions

PEFC Stack
- Membrane: 14-µm, 850 EW, PFSA Mechanically reinforced, with chemical additive
- Cathode Electrode: JMFC d-PtNi/C catalyst, 0.1 mg_{Pt}/cm^2, high surface-area carbon support, 850 EW ionomer, I/C=1.0
- Anode Electrode: Pt/C catalyst, 0.025 mg_{Pt}/cm^2, high surface-area carbon support
- Cathode/Anode GDL: Non-woven carbon paper with microporous layer (MPL), SGL 25BC, 235 µm nominal uncompressed thickness
- Seals/Frames: PET subgasket (3M patent)
- Bipolar Plates: 3-mil (0.075 mm) 316 SS substrate with Treadstone coating, 0.5 mm land, 0.7 mm channel, 0.4 mm depth. 62.5% active area, 15 $m\Omega.cm^2$ 2X ICR*

Fuel Management System
- Hybrid ejector-recirculation pump
- 35% pump efficiency, 1% H_2 purge
- 3 psi pressure drop at rated power

Air Management System
- Integrated centrifugal compressor-expander-motor module (Honeywell), air foil bearings (AFB)
- Mixed axial flow compressor
- Inflow radial expander, variable area nozzle
- 3-phase brushless DC motor, liquid and air cooled; liquid-cooled motor controller
- Efficiencies at rated power: 71% compressor, 73% expander, 89.5% motor, 89.5% controller
- Turn-down: 20
- 5 psi ΔP between compressor discharge and expander inlet at rated power

Heat Rejection System
- Two circuits: 75-95^{o}C HT, 10°C ΔT
  65^{o}C LT coolant, 5°C ΔT
- 55% pump + 92% motor efficiency
- 45% blower + 92% motor efficiency
- 10 psi ΔP in stack and 5 psi in radiator

Water Management System
- Planar cross-flow humidifier with Gore's M311.05 membrane

*2X ICR: two-sided interfacial contact resistance

Rated Power Performance of FCS with Alloy catalysts

Stack Parameters	2017 FCS with d-PtNi/C Catalyst	2016 FCS with Binary NSTF Catalyst
Membrane	Ionomer: 850 EW PFSA with chemical additive Substrate: Mechanical reinforcement Thickness: 14 µm	Ionomer: 3M 725 EW PFSA with chemical additive Substrate: 3M support Thickness: 14 µm
Cathode Catalyst	Electrode: d-$PtNi_3$ (0.1 mg_{Pt}/cm^2), acid washed Ink: organic, EW=850, I/C=1.0	d-Pt_3Ni_7 (0.095 mg_{Pt}/cm^2) with Pt/C cathode interlayer (0.016 mg_{Pt}/cm^2)
Anode Catalyst	Pt/C (0.025 mg_{Pt}/cm^2)	$Pt_{68}(CoMn)_{32}$/NSTF (0.019 mg_{Pt}/cm^2)
Stack Gross Power	88.1 kW	88.2 kW
Stack Voltage (Rated)	250 V	300 V
Number of Active Cells	377 cells (also 376cooling cells)	453 cells (also 452 cooling cells)
Stack Gross Power Density	2.84 kW/L	2.49 kW/L
Stack Gross Specific Power	3.45 kW/kg	2.99 kW/kg
Stack Inlet Pressure	2.5 bar	2.5 bar
Stack Coolant Temperature	84°C (inlet), 94°C (outlet)	83.9°C (inlet), 93.9°C (outlet)
Stack Air Inlet/Outlet RH	Inlet: 75% RH at 84°C; Outlet: 100% RH at 94°C	Inlet: 50% RH at 85°C; Outlet: 88% RH at 95°C
Stack Fuel Inlet/Outlet RH	Inlet: 42% RH at 94°C; Outlet: 100% RH at 84°C	Inlet: 43% RH at 95°C; Outlet: 105.7% RH at 85°C
Cathode/Anode Stoichiometry	1.5 (cathode) / 2.0 (anode)	1.5 (cathode) / 2.0 (anode)
Cell Area	213 cm^2 (active), 346 cm^2 (total)	208 cm^2 (active), 333 cm^2 (total)
Cell Voltage	663 mV	663 mV
Current Density	1.651 A/cm^2	1.418 A/cm^2
Crossover Current Density	4.2 mA/cm^2 @ 80°C, 100% RH, 1atm P_{H2}	5.0 mA/cm^2
Power Density	1095 mW/cm^2	941 mW/cm^2
Balance of Plant		
Humidifier Membrane Area	0.8 m^2	0.53 m^2
Air Pre-cooler Heat Duty	6.3 kW	5.7 kW
CEM Motor and Motor Controller Heat Duty	3.0 kW	3.0 kW
Main Radiator Heat Duty	78.9 kW	79.8 kW
CEM Power	Compressor shaft power: 10.3 kW Expander shaft power out: 4.7 kW Net motor and motor controller: 7.0 kW_e	Compressor shaft power: 10.4 kW Expander shaft power out: 4.7 kW Net motor and motor controller: 7.1 kW_e
Fan and Pump Parasitic Power	0.5 kW_e (coolant pump), 0.3 kW_e (H_2 recirculation pump), 0.345 kW_e (radiator fan)	0.5 kW_e (coolant pump), 0.3 kW_e (H_2 recirculation pump), 0.345 kW_e (radiator fan)

ORR Kinetics for d-PtNi/C Catalyst MEA

Distributed ORR kinetic model

- For Tafel kinetics, the ORR and CCL Ohmic overpotentials are separable

$$\eta_c = \eta_s^c + iR_\Omega^c\left(\frac{i\delta_c}{b\sigma_c}\right)$$

$$i = i_0(1-\theta)e^{-\frac{\omega\theta}{RT}}e^{\frac{\alpha nF}{RT}\eta_s^c}$$

- An optimization algorithm required to determine i_0 and ω

$$i_0 = i_{0r}e^{-\frac{\Delta H_S^C}{RT}\left(\frac{1}{T}-\frac{1}{T_r}\right)}P_{O_2}^{\gamma}\left(\frac{\lambda}{\lambda_0}\right)^{\beta}$$

- Solid solution model for PtO_x formation using cyclic voltammetry at 80^0C, 100% RH,1.5 atm, 0.5 l/s 4%H_2 & 0.5 l/s N_2, 30-min constant potential hold

$$Pt + H_2O = PtOH + H^+ + e^-$$

$$PtOH = PtO + H^+ + e^-$$

$$\theta = \theta_{PtOH} + \theta_{PtO}$$

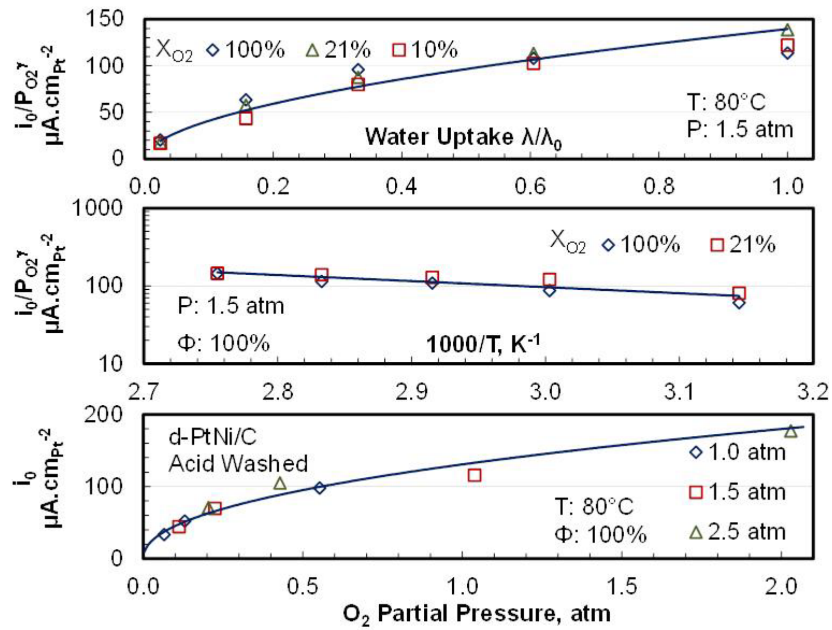

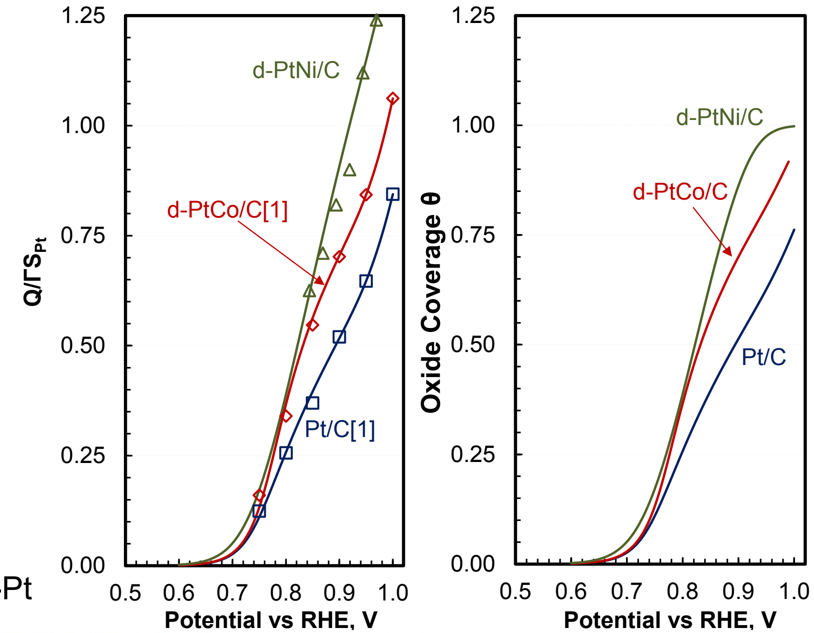

Q: Coulombs
Γ: 210 µC/cm^2-Pt

[1] Arisetty et. al. (2015). ECS Transactions, 69, 273-289

Mass Transfer Overpotential Correlation

- Mass transfer overpotentials derived from pol curves do not correlate with mass activity

$$\eta_m = E_N - E - iR_\Omega^m - \eta_c - \eta_a$$

- Product representation of i_L - current density at which η_m = 450 mV

$$i_L = i_L(P, P_{O2}) f_1(T) f_2(\Phi)$$

- Mass transfer overpotential correlation

$$\ln(\eta_m/\eta_{mL}) = F(P, T, X_{O2}, \phi, i/i_L)$$

- η_m correlation used to obtain expanded polarization data

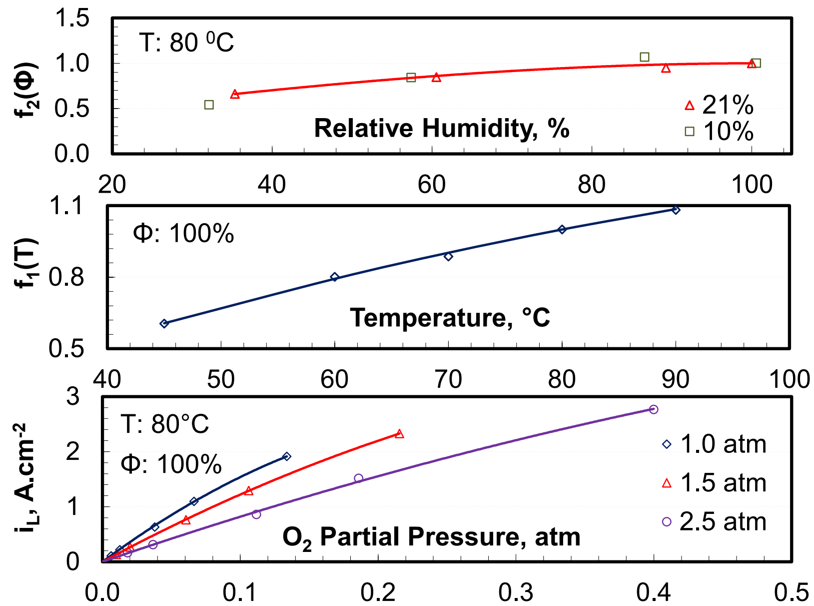

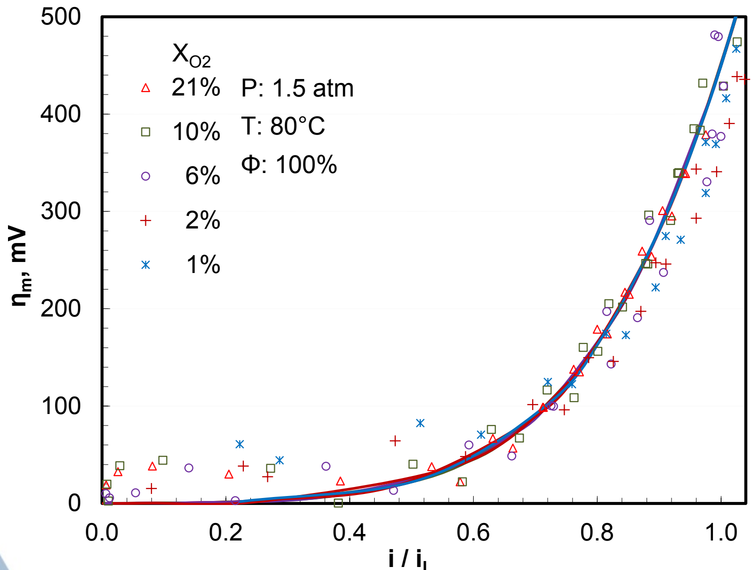

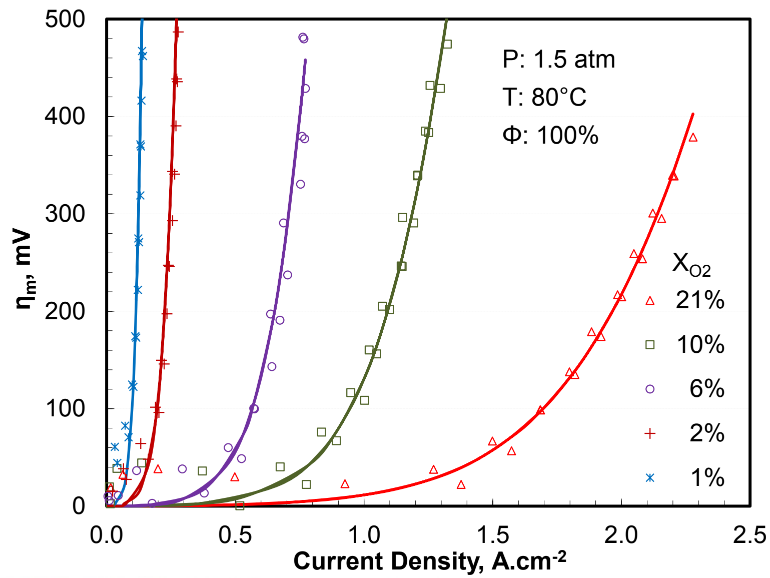

Nomenclature

a	annealed
A_{Pt}	Pt electrochemical specific area
b	Tafel slope
CI	cathode interlayer
d	de-alloyed
E	cell voltage
E_N	Nernst potential
i	current density
i_0	exchange current density
i_{0r}	reference exchange current density
i_L	limiting current density
L_{Pt}	Pt loading
n	no of electrons
P	pressure
R	gas constant
R_{cf}	CCL O_2 transport resistance
R_{cs}	cell to stack additional resistance
R_d	GDL O_2 transport resistance
R_g	gas channel O_2 transport resistance
R_m	mass transfer resistance
R_Ω^c	cathode ionic resistance
R_Ω^m	high-frequency resistance (HFR)
RH	relative humidity
SR	stoichiometry
S_{Pt}	Pt surface roughness
T	temperature
T_r	reference temperature, 353 K
X	mole fraction
ΔH_s^c	ORR activation energy
α	symmetry factor
β	relative humidity dependence
γ	O_2 partial pressure dependence
δ_c	cathode electrode thickness
δ_d	GDL thickness
δ_l	liquid layer thickness
ε_i	ionomer volume fraction
ε_τ^d	ε/τ in dry portion of GDL
ε_τ^w	ε/τ in wet portion of GDL
η_a	anode overpotential
η_c	cathode overpotential
η_m	mass transfer overpotential
η_s^a	HOR kinetic overpotential
η_s^c	ORR kinetic overpotential
θ	oxide coverage
λ	water uptake
σ_c	cathode ionic conductivity
σ_m	membrane conductivity
τ	tortuosity